A New Method for Spike Extraction Using Velocity Selective Recording Demonstrated with Physiological ENG in *Rat*

B.W. Metcalfe[a,*], D.J. Chew[b], C.T. Clarke[a], N. de N. Donaldson[c], J.T Taylor[a]

[a]*Department of Electronic and Electrical Engineering, University of Bath, Bath UK*
[b]*John Van Geest Centre for Brain Repair, Department of Clinical Neuroscience, University of Cambridge, Cambridge UK*
[c]*Department of Medical Physics and Biomedical Engineering, University College London, London UK*

Highlights

- **New methods are developed to extract spike trains based on conduction velocity.**
- **Histograms describing firing rates of particular neurons are created.**
- **Methods are applied to data recorded in-vivo from rat.**
- **Cutaneous skin sensation is detectable from neural recordings.**

Abstract

Background **This paper describes a series of experiments designed to verify a new method of electroneurogram (ENG) recording that enables the rate of neural firing within prescribed bands of propagation velocity to be determined in real time. Velocity selective recording (VSR) has been proposed as a solution to the problem of increasing the information available from an implantable neural interface (typically with electrodes in circumferential nerve cuffs) and has been successful in transforming compound action potentials into the velocity domain.**

New Method **The new method extends VSR to naturally-evoked (physiological) ENG in which the rate of neural firing at particular velocities is required in addition to a knowledge of the velocities present in the recording.**

Results **The experiments, carried out in rats required individual spikes to be distinct and non-overlapping, which could be achieved by a microchannel or small-bore cuff. In these experiments, strands of rat nerve were laid on ten hook electrodes in oil to demonstrate the principle.**

Comparison with Existing Method **The new method generates a detailed overview of the firing rates of neurons based on their conduction velocity and direction of propagation. In addition it allows real time working in contrast to existing spike sorting methods using statistical pattern processing techniques.**

Conclusions **Results show that by isolating neural activity based purely on conduction velocity it was possible to determine the onset of direct cutaneous stimulation of the L5 dermatome.**

Keywords: Velocity Selective Recording, VSR, Spike Sorting, ENG, Velocity Spectral Density

1. INTRODUCTION

If it were possible to construct an ideal nerve interface, such a system would allow recording from and stimulation of every single axon in the nerve; it would be stable in time so that each axon, once identified, would have a known function. Every axon would have a physiological label so, for example, some axons in the femoral nerve, after identification, would be labelled *vastus lateralis, efferent*. However, before these physiological labels could be attached, it would be helpful to know the propagation velocity and direction for every fibre (*afferent* or *efferent*) which would greatly reduce its possible range of function. At present of course, no such interface exists. Practical methods start with the axon-specific, such as intra-fascicular devices, fine tungsten needle electrodes (Yoshida et al. 2000) or arrays such as the Utah design (Maynard et al. 1997); these are typically invasive, show poor chronic applicability in peripheral nerves, and give no indication of the axon/action potential characteristics. At the extra-fascicular level, *cuffs* can be safe for chronic clinical use, but are limited in recording the composite activity from all the axons in the nerve. In this range of types, *Longitudinal Intrafasicular Electrode* (LIFE) arrays can record from small groups of axons, perhaps within one fascicle, but do not show activity in the whole nerve (Boretius et al. 2010). Micro-channel nerve interfaces have enabled inter-fascicular recording from peripheral nerves with single unit activity resolution, but the number of axons in each micro-channel is quite large (~100 (FitzGerald et al. 2012)) and physiological characterisation is still limited. No current interface method allows communication with one axon, or even a group of only a few axons, with physiological labelling.

The method that we call *velocity selective recording* (VSR) has been applied to cuffs and, by extension, could be applied to micro-channels. By filtering the neural signal in the *velocity domain*, activity within bands of conduction velocity can be discriminated and, if that band corresponds to a functional group of fibres, such as, for example, the *γ efferents* which are responsible for muscle spindle contraction, it should be possible to estimate the activity in those fibres. Thus the VSR method should improve both the quantity and quality of the information that can be extracted from the neural signal using practical types of electrode structure. This improvement may yield substantial benefits in a clinical neuroprosthesis if one can provide better resolution at the input. However, in spite of the many potential applications of VSR, to date it has only been demonstrated with electrically-evoked electroneurogram (ENG), i.e. *compound action potentials* (CAPs) (Schuettler et al. 2011), (Schuettler et al. 2013). This is because there are several very significant differences between

the requirements of recording electrically-evoked and natural ENG that complicate the process of recording the latter. These differences include much smaller signal amplitudes (typically, using cuffs, 1 - 10 μV, as opposed to about 100 μV for CAPs) and the need to determine the rate of neural firing in a particular velocity band, rather than the relative amplitudes of activity between bands, which is generally the case for CAPs. This paper presents the first experimental validation of a new VSR-based method using naturally - evoked (physiological) signals. The data were obtained from a strand of intact nerve within a dorsal/sensory root of a *rat* and a new method was employed that overcomes the difficulties of recording natural ENG and allows neuronal firing rates in specified velocity bands to be computed in real time. We call this the method of *velocity spectral density* (VSD) (Metcalfe et al. 2014).

The new method was validated by capturing and then manually calculating the propagation velocities of individual spikes (i.e. *action potentials*-APs) and comparing the firing rates in each of a chosen set of velocity bands with the output from the VSD processor. The recording was made with the nerve resting on hook electrodes immersed in oil. This was convenient for the experiment but we expect that the signals so obtained were similar to the outputs from a row of electrodes in a micro-channel. Both arrangements greatly increase the amplitude of extracellular potentials (V_{ex}) compared to a nerve of diameter 1 mm or greater placed in a cuff, enabling individual ENG spikes to be distinguished and counted: this is essential for the method and also allows validation by inspection of the electroneurograms. The ten electrodes were connected in separate pairs to form five *bipolar* recording channels before amplification and band-pass filtering.

There is, of course, a long history of analysing neural recordings from microelectrodes in *brain*. These methods normally identify spikes by the characteristics of their shape. This *spike sorting* is generally not done in real time and the methods often use substantial computing power (Gibson et al. 2012). By comparison, the proposed VSD method, in common with other VSR-based approaches, can operate in real time and is relatively economical in terms of computational effort. These features are important in certain neuroprosthetic devices such as the "Bioelectronic Medicines" currently being advocated by GlaxoSmithKline (Famm et al. 2013). This is because the devices must be small and low-powered and the firing rates of fibres that serve different functions must be calculated without significant computation delays.

Section 2 considers the VSR approach in general and the modifications and new methods necessary for it to compute VSDs while section 3 describes the experimental methods employed. Section 4 describes the experimental results and Section 5 provides discussion and conclusions.

2. Velocity Selective Recording Methods

1. *Delay-and-Add*

The essence of VSR is a simple process called *delay-and-add* that is analogous to beam-forming algorithms used in certain types of synthetic aperture arrays (Huang and Miller 2004). The channels are delayed relative to the last channel V_{B1} by an interval that depends on both the electrode spacing and the propagation velocity of the signal. So if the delay between the first two channels (V_{B1}, V_{B2}) is *dt* the delay between the first and third channels (V_{B1}, V_{B3}) is $2 \cdot dt$ and so on. The general index of this process is i and $1 \leq i \leq C$ where $C.dt$ is the maximum delay of interest. Delay-and-add operates by inserting delays into the channels to effectively cancel the naturally-occurring delays, after which the channels' outputs are summed resulting in a single signal V_D (Equation 1) as illustrated in Figure 1 (Schuettler et al. 2011).

$$V_D[n, dt] = \sum_{i=1}^{C} V_{Bi}[n - (i-1) \cdot dt] \qquad \ldots(1)$$

Where C is the number of recording channels and n is the current sample index. For each velocity of interest, a corresponding value of *dt* is applied, so that there are many (m) data

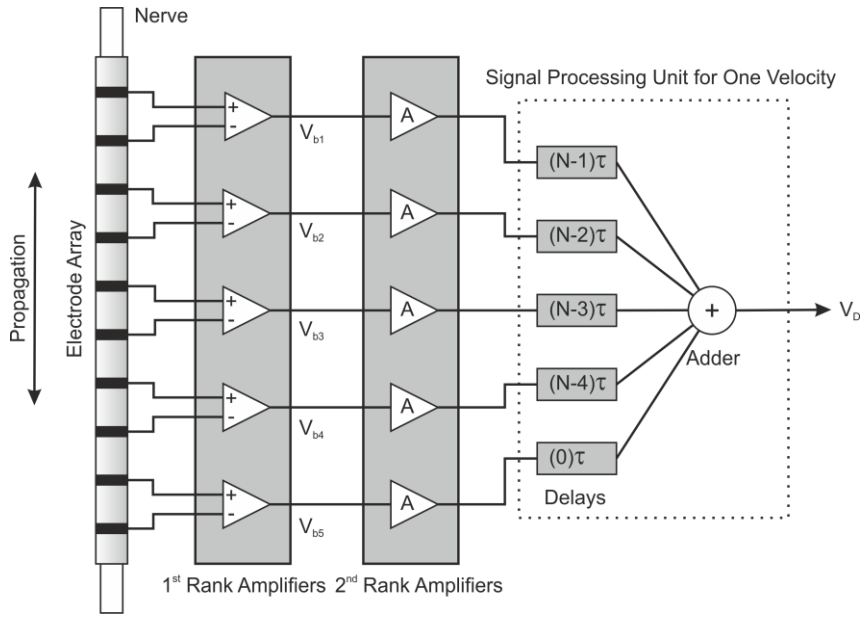

Figure 1: The basic concept of delay-and-add showing the signal processing requirements for one velocity. The signals are differentially amplified before being artificially delayed and summed together. The delay units required differ from one velocity to another.

streams after the addition operation, each of which corresponds to a different conduction velocity. One advantage of VSR is the ability to record and isolate neural activity that is both *afferent* and *efferent* by simply applying a negative value of *dt* during the delay process; however this has yet to be experimentally verified and was not relevant to the data in this study. Furthermore, when delay-and-add is used and the noise sources are uncorrelated then there is an increase in SNR of approximately $\sqrt{C}$ (Donaldson et al. 2008). This property can be exploited to identify APs that may not be directly observable in the time records of the individual channels and thus could not be classified by traditional spike sorting methods.

2. *Velocity Spectral Density*

To date the principle of VSR has been applied to acute *in-vivo* recordings from *pig* (Schuettler et al. 2011) and *frog* (Schuettler et al. 2013) where the nerve fibres have been selectively recruited using electrical stimulation. In contrast to natural activation, electrical stimulation recruits, approximately simultaneously, every axon within the nerve for which the stimulation current is supra-threshold. Electrical stimulation therefore produces a CAP that describes the excited population. The *intrinsic velocity spectrum* (IVS) is found by varying *dt* and taking the peak of the response as a measure of the number of fibres that were excited at the corresponding velocity (Schuettler et al. 2013). However this approach does not, by itself, result in a method to measure the firing rate for axons of particular velocities, which is of

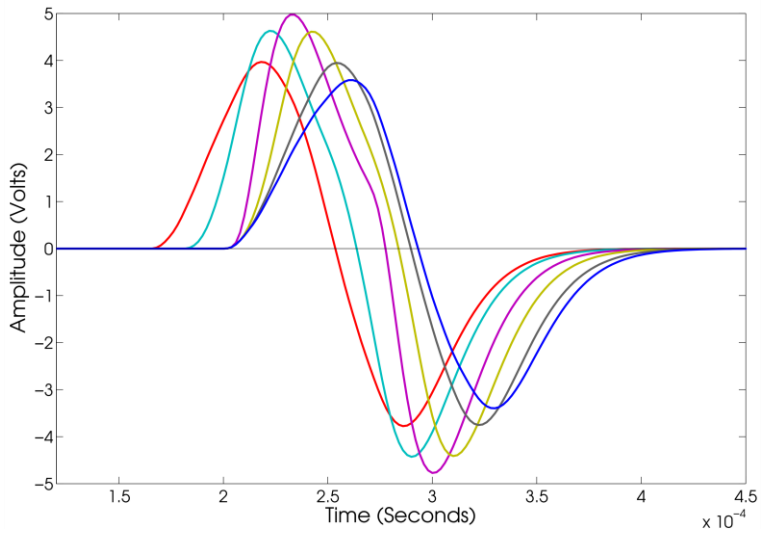

Figure 2: Typical V_D waveforms for a single AP. Five channels of data (containing a single AP propagating at 15 m/s) have been delayed and summed for values of delays corresponding to velocities of 13 - 17 m/s from left to right respectively. It is clear to see the effects of constructive superposition at the matched velocity, the largest positive and negative peak occurs at the delay corresponding to the conduction velocity.

interest when analysing physiological ENG.

One method for extracting both conduction velocity and neuronal firing rates from a nerve recording is to use a sliding time window of sufficient length to enclose only a single AP. Delay-and-add can then be applied to extract the IVS of the window contents and thus identify the most likely conduction velocity for the AP based on the velocity of the peak value, V_{peak}. This process could be repeated as the window is moved along the time record and the firing rates extracted by simply counting the number of occurrences of each velocity but this has two significant drawbacks. Firstly, the window must only contain a single AP, otherwise only the AP with the largest amplitude will be identified as the largest peak in the IVS. Secondly the windowing function must be carefully selected to avoid *velocity spectral leakage* (VSL), an effect that is similar to spectral leakage in the frequency domain, resulting from the time domain window failing to encompass the AP fully. A more robust method has been developed that does not require the use of a sliding time window and so avoids these issues. The new method by which both conduction velocity and neuronal firing rates can be extracted is termed the method of *velocity spectral density* (VSD) and can be described in the following steps.

Delay-and-Add. A set of C time records of arbitrary length is processed using the delay-and-add method as described above to generate a set of m, V_D waveforms (see Equation 1). The values of dt used can be selected, based on the required velocity range and resolution. For example a velocity range of 10 - 50 m/s with an electrode spacing of 1 mm requires dt values in the range 20 - 100μs. If the resolution is 1 m/s, m = 41. An example is shown in Figure 2 where five channels of raw data containing a single AP propagating at 15 m/s have been summed together with a values of dt corresponding to velocities of 13, 14, 15, 16, 17 m/s.

Centroid Gating. In order to identify an AP the relationship between V_D for neighbouring values of dt must be examined. Each V_D waveform is passed through a filter that detects the centroid of each AP (Metcalfe et al. 2014). This filter is implemented as a linear *finite impulse response* (FIR) filter with impulse response $h[n]$:

$$h[n] = -\frac{2}{N}n + 1 \quad \ldots (2)$$

This is a linear function of gradient -2/N where N is the width of the filter and n is the current index of the discrete-time samples. The function $h[n]$ varies in amplitude from +1 to -1 where N is chosen to be at least as wide as a single AP in the time domain. Since in

practice the AP is neither regular nor symmetric the centroid represents a more robust method for locating the midpoint of the AP than taking the maximum value. The centroid can be considered as the geometric centre of any two dimensional region, in this case the area under the AP as bounded by the *x* axis. It is necessary to separate the positive and negative phases of the AP before locating the centroid, and this was achieved *via* half wave rectification of the signal. It is assumed throughout that there is zero DC offset in the data (in practice this was achieved by band-pass filtering the data). Computing the centroid considers the contribution from every sample as opposed to the single samples used in peak detection and so it is more robust against noise and interference. The filter output can now be described by $y[n, dt]$ which is the convolution of $h[n]$ with $V_D\,[n, dt]$:

$$y[n, dt] = \sum_{k=-\infty}^{\infty} \left[\left(-\frac{2}{N}(n-k) + 1 \right) \cdot \left(\sum_{i=1}^{C} V_{Bi}(n - (i-1) \cdot dt) \right) \right] \quad \ldots(3)$$

$y[n,dt]$ passes through zero at a point that corresponds to the centroid of each AP time shifted by the group delay of the filter T_g, which, due to negative symmetry in the impulse response, is given by:

$$T_g = (N-1)T/2 \quad \ldots(4)$$

Where T is the sampling interval and N is the filter order. Whenever a zero-crossing is detected, the instantaneous value of V_D is held (Figure 5):

$$V_D(n, dt) = \begin{cases} y[n, dt], & y[n-1] > 0 > y[n+1] \\ 0, & otherwise \end{cases} \quad \ldots(5)$$

The process is illustrated by the example shown in Figure 3. For clarity, continuous-time variables are used and $h(t)$ is shown in the upper part of the figure while the AP is represented by a unit square pulse ('top hat' function) $x(t)$ shown dashed below. N is taken to be 1.5, i.e. 1.5 times the width of the unit pulse. Convolving the two functions (i.e. applying the continuous-time version of Equation 3) and shifting the output using Equation 4 results in the function $y(t)$, which is also shown in the lower plot in Figure 3. As can be seen, the zero crossing of $y(t)$ passes through the point $t = 0$, coinciding with the centroid of the pulse. The effect of using the method with a real AP as recorded from *rat* is shown in Figure 4.

Detection Criteria

A detection algorithm can now be used that examines each velocity response $V_D[n, dt]$ for the criteria $V_{D-1} < V_D > V_{D+1}$. The held value of $V_D[n, dt]$ is compared to a noise threshold, calculated from measurements of the input-referred noise floor, and then compared across the *m* data streams. As shown in Figure 5 the gated centroid of each $V_D[n, dt]$ waveform is offset in time by a multiple of the sampling interval and so the examination of each response is not trivial. In order to compare the amplitudes the value of each gated waveform is held in memory until the next AP occurs, i.e. when the gated value of $V_D[n, dt]$ is next non-zero. It is then straightforward to compare the values stored in memory. If this criterion is met then an AP has been detected with a peak conduction delay (and thus velocity) of *dt* and the corresponding histogram bin can be incremented accordingly.

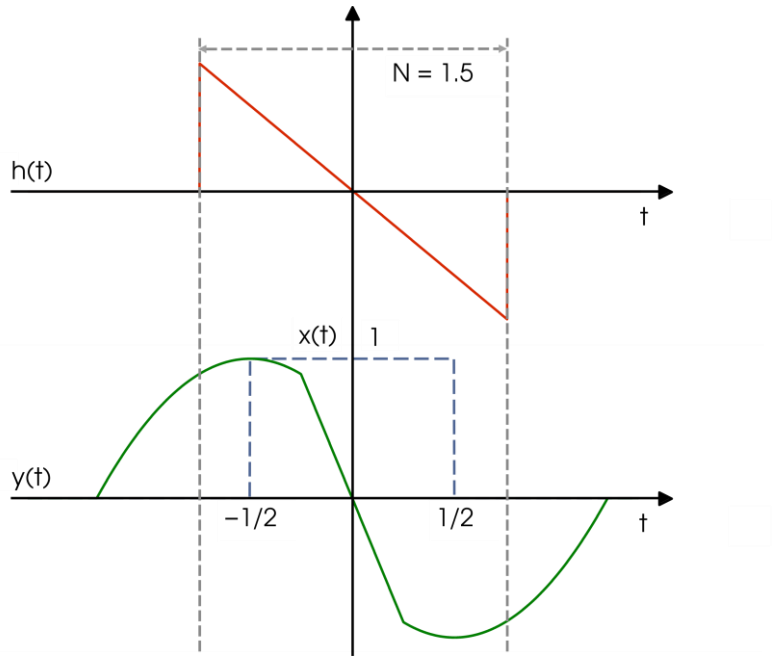

Figure 3: An example to illustrate the calculation of the centroid of an AP using the FIR filter $h[n]$. For clarity, h is represented by the continuous-time function shown in the upper plot in the figure while the 'top hat' function shown in the lower plot represents the AP. Application of the convolution and shift functions results in the output function y(t) whose zero crossing corresponds with the centroid of the 'top hat' function.

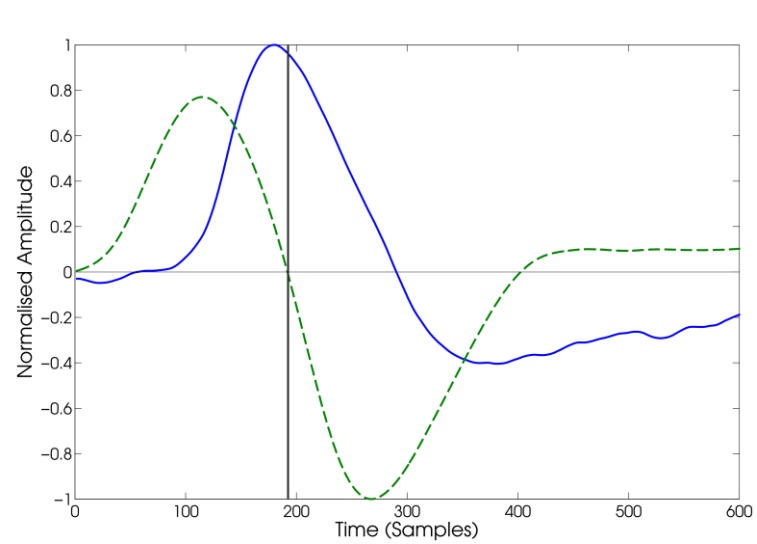

Figure 4: The application of the centroid filter to a single channel of data containing a realistic AP. In this case the width of the centroid filter was chosen to be N = 100 samples, or approximately the width of the positive phase of the AP. The solid line represents the input waveform, $V_D[n]$, and the dashed line the filter output $y[n]$. The vertical marker is set at the negative-going zero crossing of the filter output and is located at the centroid of $V_D[n]$.

3. Experimental Methods

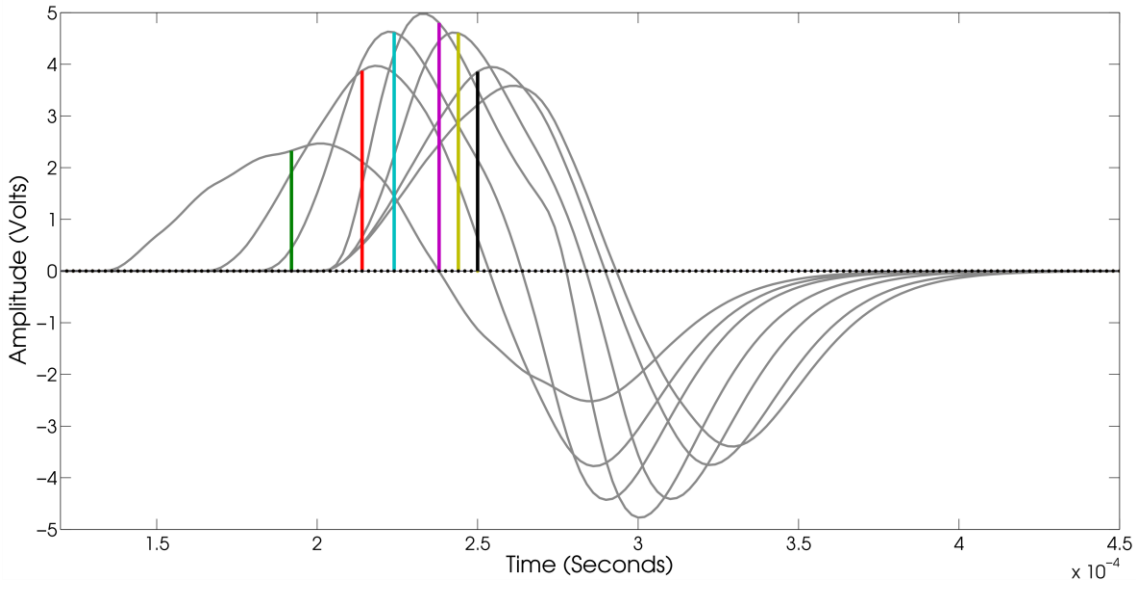

Figure 5: Using the output from each centroid filter the V_D data steams may now be gated (or held) for single sample values at the centroid of each AP. The resulting spikes (which are superimposed on the original V_D waveforms) may now be inspected for the detection criteria. In this case it is clear that the most likely conduction velocity occurs for a value of V_D corresponding to 15 m/s, the range of velocities is 13 – 17 m/s from left to right respectively.

3. Surgical Procedure

All animal procedures were performed in accordance with the United Kingdom Animal (Scientific Procedures) Act 1986. An adult female Sprague Dawley *rat* (250 grams) was anaesthetised with 1.5 g/kg urethane (Sigma) administered by the *intraperitoneal* route. The dorsal spinal cord was exposed *via* a laminectomy of three of the lumbar spinal vertebrae. The dorsal skin was sutured to an over-hanging rectangular bar, creating a contained pool into which non-conductive mineral oil was poured. The *dura* was incised to expose the dorsal roots.

The left fifth lumbar dorsal root (L5) was micro-dissected into fine rootlets/fascicles with fine glass pulled pipettes, in a method described previously (Chew et al. 2013),(Delivopoulos et al. 2012),(Minev et al. 2012). The dorsal root was chosen for a number of reasons. Firstly it is long enough to fit in the multiple electrode array; secondly it is amenable to the micro-dissection technique, and finally it is exclusively sensory. During the course of the experiment, modulation of the neural signals was elicited by stimulating the L5 dermatome both manually (*via* direct cutaneous touch) and electrically (*via* bipolar pin electrodes).

One fascicle, approximately 100 µm in diameter, was placed over all of the hooks in the array. The electrodes were arranged in a shared bipolar configuration whereby five channels were recorded from ten independent but commonly-referenced amplifiers in a multiple electrode structure, a simplified recording diagram is illustrated in Figure 6 (Taylor et al. 2004). The amplifiers were connected to the recording set-up (Digitimer, UK) and the animal was suitably electrically grounded to the recording equipment and the surrounding Faraday cage. The ten hooks were connected to five unity-gain head-stages (Neurolog NL100) numbered in the orthodromic direction of propagation. Following each head-stage, the signal was pre-amplified 1000 times using an AC-coupled amplifier (Neurolog NL104A), fed through a 50 Hz interference eliminator (Humbug, Quest Scientific, Canada) and amplified 10 times further (Neurolog NL106) before band pass filtering at 300 - 5,000 Hz. The total system gain was 80 dB.

4. Recording and Stimulation Electrodes

The recording electrode array was fabricated on site, having ten hooks joined to an insulating bar that was supported by a clamp stand. Each hook was formed from 0.2 mm diameter tungsten wire fed through a polyurethane tube of 0.4 mm (internal) diameter. Each wire was fixed in its tube by cyanoacrylate adhesive. The hooks were formed at one end by winding

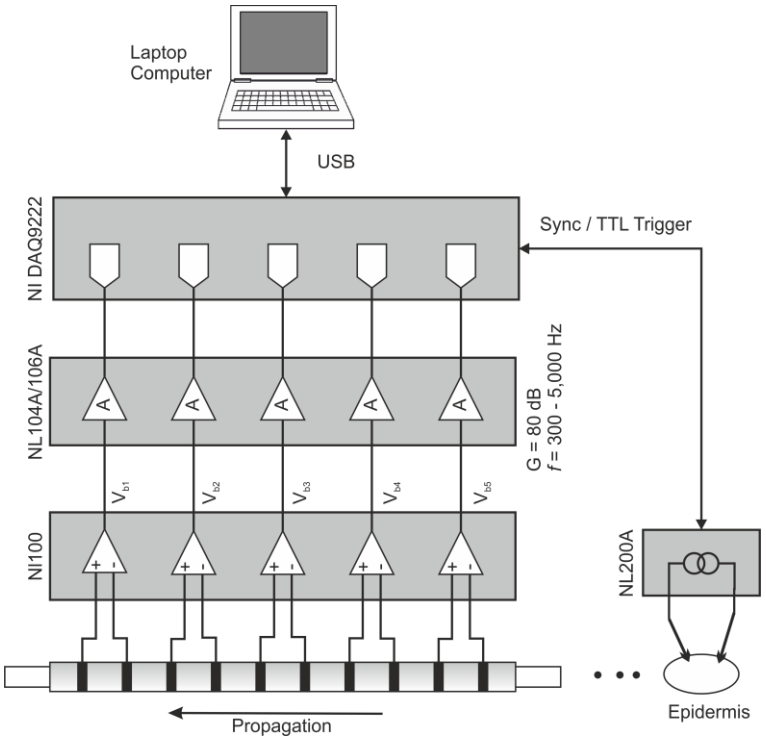

Figure 6: Recording setup used to acquire physiological ENG. A bank of Digital to Analogue converters were used to digitise five channels of data simultaneously. The stimulation was controlled by the laptop computer via the data converters using a TTL pulse. The stimulation electrodes were inserted into the dermis distally from the recording electrodes.

around a cylinder of 4 mm diameter; the shape of each hook was then maintained by the rigidity of the wire. The total length of the electrode array was 5 mm.

In addition to the array of recording electrodes, a further pair of *pin* electrodes was applied to the fifth lumbar (L5) dermatome for electrical stimulation of the skin. The purpose of this was to test the recording system at the start of the experiment and to show the CAP from the cutaneous afferents that will include the touch receptor fibres. The pin electrodes were connected to a Neurolog NL200A stimulus isolator driven from an NL301 pulse generator. Square wave stimulation pulses were applied with varying currents (0.3 mA to 4 mA) but with a constant width of 100 μs. The recording equipment was started by means of a synchronisation pulse that was triggered 100 μs before the application of the electrical stimulus.

5. *Data Acquisition*

The amplified and filtered signal was passed to a set of high-speed successive-approximation ADCs (NI9222 mounted in cDAQ-9178 by National Instruments, Austin, TX, USA)

providing simultaneous sampling of all five bipolar recordings with 16 bit resolution. The specifications of the converters are provided in Table 1.

TABLE 1

Property	Value
Gain Drift	6 ppm/°C
Offset Drift	29 µV/°C
CMRR (f = 60 Hz)	100 dB
-3 dB Bandwidth	>500 kHz
Input Impedance	> 1GΩ
Noise	0.75 LSB
THD (20 Vpp at 10 kHz)	-85 dB
Crosstalk (20 Vpp at 1 kHz)	-100 dB

The converters were connected to a battery operated portable laptop computer running LabView 2010 that logged each channel into a set of data files for offline analysis, no processing was performed on the data during the experiment. Each data file contained a time record and five channels of raw data corresponding to each amplifier output. On-line visual verification was provided by connecting a set of oscilloscope channels at the converter inputs; this provided a means to examine each recording in real time for conspicuous artefacts or noise.

E. Data Processing

Offline data analysis was performed using MATLAB R2012b (The MathWorks, Natick, MA, USA). Each of the five bipolar signals was sampled for 250 ms in consecutive recordings for 2.5 seconds at a sample rate of 500 kS/s. The smallest possible delay was therefore 2 μs corresponding to a maximum velocity of 1 mm / 2 μs = 500 m/s and allows for a velocity resolution of 0.2 m/s at a velocity of 10 m/s. Each bipolar signal was time-shifted against the others by multiples of *dt* and then summed to form a single signal. Where the required delay was not a multiple of *dt*, each bipolar signal was time shifted by alternating values of *dt* such that the average delay over all five channels was the desired value. VSR was used to extract the basic velocity information from the raw data, each recording lasting 250 ms in this case (Taylor et al. 2012), (Taylor et al. 2011).

4. RESULTS

6. *Electrical Stimulation*

Electrical stimulation was applied to the L5 dermatome to test the recording system and record the CAP from the cutaneous afferents. The stimulation waveform was a fixed width (100 μs) square pulse of variable amplitude and Figure 7 shows the resulting time domain response, the IVS and the V_D waveforms for the peak stimulation current of 4 mA (of length 10 ms). The location of the peaks within the IVS for each stimulation current is given in Table 2.

TABLE 2

Stimulation Current (mA)	0.3	0.5	1	2	4
Peak Populations (m/s)	10	9, 14	10	10, 14	7, 14

At lower stimulation currents the peak velocities are at approximately 10 m/s and 14 m/s and as the stimulation current is increased to 4 mA populations at lower velocities (7 m/s) are recruited in accordance with the principle of *inverse recruitment* (Carp et al. 2003). Note that during stimulation with 1 mA and 4 mA the selectivity of the system was not high enough to isolate the populations at 14 m/s and 10 m/s respectively. Figure 7 illustrates this principle, the peak at 10 m/s has been masked by the larger amplitude occurring at 14 m/s.

7. *Naturally Evoked (Physiological) ENG: Resting State*

Recordings were made using the same experimental set-up as for electrically-evoked stimulation while the animal was in a resting state, i.e. with no external stimulation applied. Ten recordings of duration 250 ms were made at 30-second intervals. The input-referred

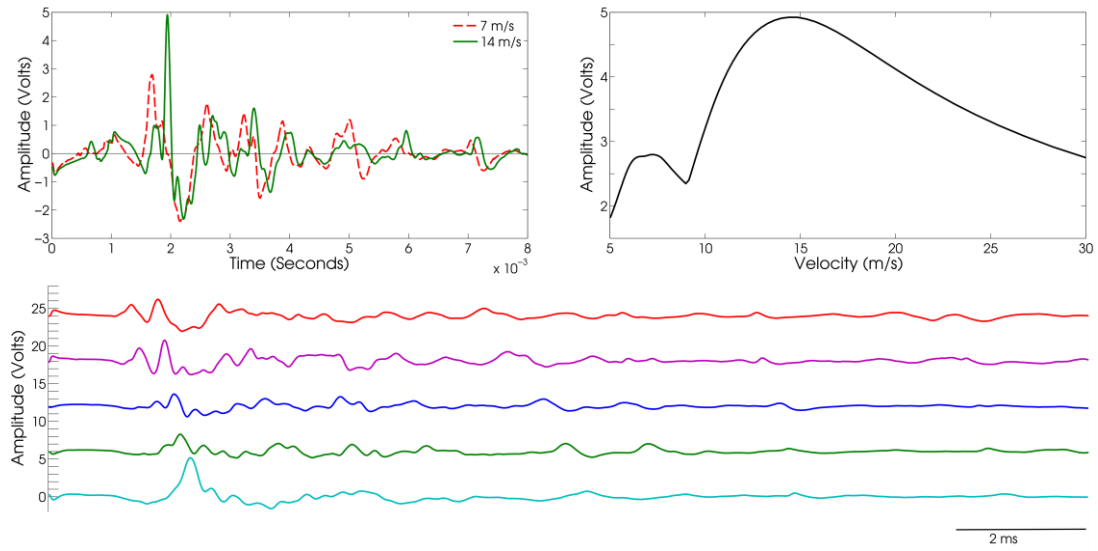

Figure 7: Electrical stimulation of the derma at 4 mA, the time domain recording (bottom inset) is synchronised with the stimulation pulse and offset by 1 ms. The dominant conduction velocities are at 7 and 14 m/s as illustrated by the IVS (right insert). The V_D waveforms corresponding to the peak velocities of 7 and 14 m/s (left inset) show the location within the time domain of these dominant peaks. The ordinate scale in each case represents signal amplitudes after total system gain of 80 dB.

noise floor was measured during a 5 ms period of no observable neural activity and ranged from 4.04 μV_{rms} to 7.31 μV_{rms} over the five channels. The observed peak-to-peak (pp) amplitudes for single APs were in the range 33.34 μV_{pp} to 65.49 μV_{pp} with larger amplitudes observed for the faster APs as is to be expected based on theoretical models (Pearson et al. 1970). SNR values (pp/rms) were therefore in the range 13.2 dB to 24.2 dB.

Figure 8 a) shows the VSD (or number of APs within each velocity band) for all of the recordings in the resting state. The VSD was computed using the mean level of activity as measured in each of the ten recordings. Error bars were fitted showing the standard deviation from the mean level of activity from all ten recordings. As already noted the majority of neural activity falls in the range 5 - 20 m/s and so the analysis has been restricted to this range (a velocity step of 1 m/s has been employed throughout). The VSD histogram clearly indicates a bi-modal peak. The two dominant peaks are located at 10 m/s and 12 m/s respectively with a consistent dip in activity at 11 m/s seen in each recording. The average number of APs identified during each 250 ms recording was 160 with a standard deviation of 7.95 APs.

8. Naturally Evoked (Physiological) ENG: Cutaneous Skin Sensation

Recordings of cutaneous skin sensation were made while lightly stroking the L5 dermatome. As in the resting state, 10 recordings of duration 250 ms were made at 30-second intervals. The input-referred noise floor was measured once again during a 5 ms period of no observable neural activity and the measured values ranged from 4.00 μV_{rms} to 8.31 μV_{rms}. The peak-to-peak signal values for a single AP were in the range of 34.95 μV_{pp} to 86.49 μV_{pp} corresponding to SNR values of 12.5 dB to 26.7 dB. These values are very similar to the previous measurements.

Figure 8 b) shows the VSD histogram for the recordings made with cutaneous stimulation of the L5 dermatome. These are in the same format as Figure 8 a), for the resting case. Since the

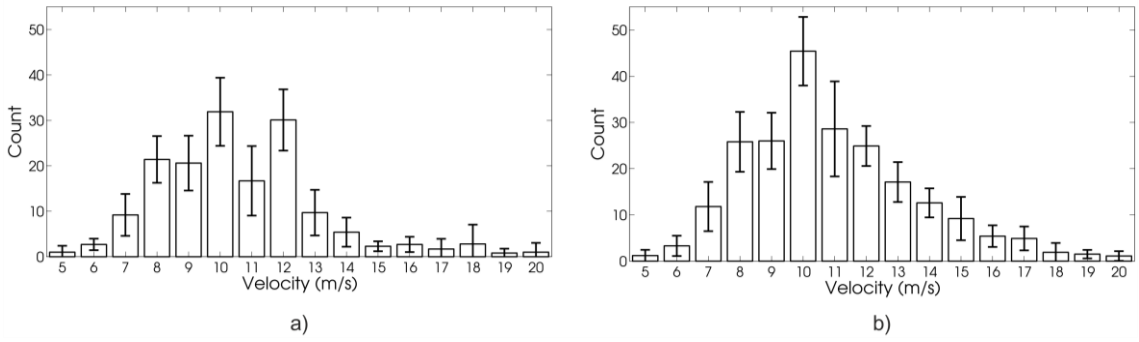

Figure 8: VSD histograms computed for each 2.5 second composite recording made without (left) and with (right) manual stimulation of the derma. The VSD is shown with mean activity levels for each velocity band, error bars show the standard deviation from all ten recordings.

exact location of the stimulation event within the time record was unpredictable, each recording was inspected visually to ensure that one (and only one) event had been captured. The VSD histogram in Figure 8 b) clearly indicates that the distribution of axon firing has changed from a bi-modal distribution to a single peak located at 10 m/s. The average number of APs identified during each 250 ms recording was 220.7 with a standard deviation of 27.07 APs (compared to 160 with a standard deviation of 7.95 APs for the resting state).

9. Validation

In order to validate the VSD process the conduction velocities of 50 APs selected at random were measured in the time domain by hand, the average delay as measured from the peak of the AP from one channel to the next was used to compute the conduction velocity. The results were compared with the output from the VSD processor. In all cases there was exact agreement between the conduction velocities measured by the two methods.

10. Spike Density Functions

An alternative method of presenting the output of the VSD process is to plot the time record of the output of the VSD gating function (aka a spike train). This was done for both the resting and stimulated data and the results are shown in Figure 9. Since the outputs are velocity dependent, a velocity of 10 m/s was chosen since earlier experiments demonstrated a clear increase in apparent firing rate during stimulation at that velocity. In order to represent the spike train as a continuous function, the spike train was convolved with a smooth and continuous kernel function (Szűcs 1998).

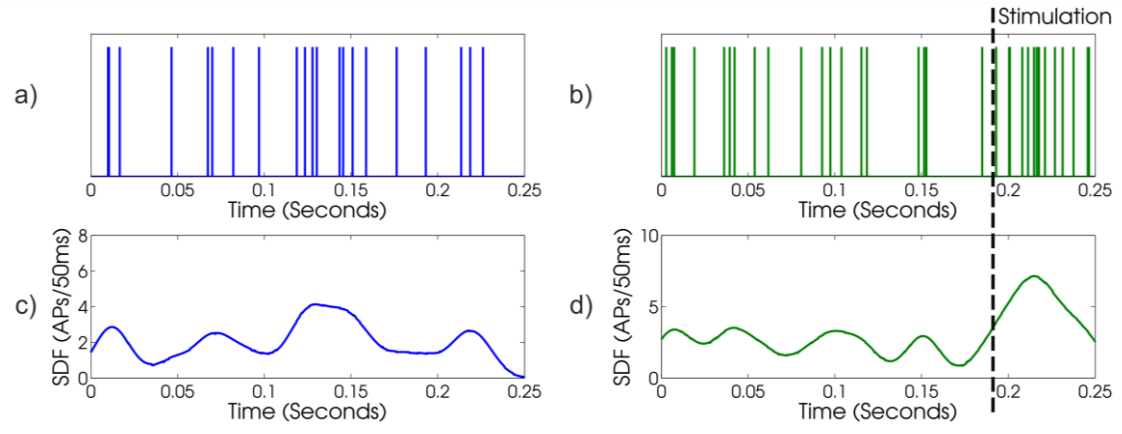

Figure 9: Spike trains (top) and spike density functions (bottom) for APs propagating at 10 m/s over a 250 ms recording with (right) and without (left) manual stimulation of the derma. The start of the stimulation event is indicated in the figure and corresponds to a visible increase in firing rates at a conduction velocity of 10 m/s.

Figures 9 a) and b) show the spike trains for APs propagating with a velocity of 10 m/s with and without cutaneous stimulation of the L5 dermatome respectively. The stimulation event occurred at approximately 200 ms from the start of the second recording. Figures 9 c) and d) show the smoothed spike trains, smoothed by convolution with a normalised Gaussian window 50 ms in length. Both recordings show an oscillatory background firing rate, approximately limited to between 1 and 4 APs per 50 ms. At the onset of stimulation there is a large jump in the firing rate to approximately 7 APs per 50 ms.

5. Discussion

11. Validity of Results

Within the nervous system, information is encoded in terms of neuronal firing rates and so an increase in the amplitude of the stimulus results in a correlated increase in the rate of AP generation (Milner-Brown et al. 1973). As an example, the *afferent* fibres that contain information about the fullness of the human urinary bladder have been observed in *man* to propagate at a mean velocity of 41 m/s with a base-line firing rate of about 15 APs per 200 ms and a rate representing a full bladder of about 400 APs per 200 ms (Schalow et al. 1995).

In order to evaluate the statistical significance of the variation between the individual experiments a paired *t* - test was performed using all available data for each velocity band (O'Mahony 1986). Data from the resting and cutaneous stimulation experiments were compared and the results are given in Table 3 (the threshold for the null hypothesis was set to 5%). The variable **P** represents the probability of observing a test result as extreme as the observed value if the null hypothesis is true. **H** is a Boolean variable indicating rejection of the null hypothesis when **H** is set to 1. The null hypothesis was rejected for the velocities in the range 10 m/s - 17 m/s suggesting that the cutaneous stimulation produced an observable change within these velocity bands.

TABLE 3

Velocity	**5**	**6**	**7**	**8**	**9**	**10**	**11**	**12**	**13**	**14**	**15**	**16**	**17**	**18**	**19**	**20**
P (%)	78	44	22	22	8.6	0.2	1.6	0.7	0.5	0.1	0.3	2.2	0.3	58	17	89
H	0	0	0	0	0	1	1	1	1	1	1	1	1	0	0	0

The velocity band 10 m/s - 17 m/s is within the accepted range of conduction velocities for the $A\delta$ (5 - 30 m/s) *afferent* fibres in *rat*, which are responsible for light touch sensation (Gasser 1941). Typically motor signals would be carried by *efferent* fibres however because the signals recorded within this study were purely *afferent* in nature, the most likely candidate for the source of the increased activity is the $A\delta$ group of sensory nerve fibres.

During each recording there was some observed variability of both the signal and noise amplitudes from one electrode channel to another. The most likely explanation for this is the variation in extracellular resistance along the length of the fascicle that can affect the amplitude of the recorded signals (Rahal et al. 2000). When using cuffs or micro-channels the position of the nerve is tightly constrained and so the inter-electrode impedances are fairly consistent along the array. This is not the case with simple wire hook electrodes where the nerve is only resting on each hook and so the longitudinal extracellular impedance was likely to have been quite variable along the array.

12. Interference and Noise

Tripolar recording has been shown to reduce common mode interference signals such as the *Electromyogram* (EMG) that are typical of *in vivo* recordings of this nature (Donaldson et al. 2008). In this study the use of insulating mineral oil around the fascicle and the application of a band pass filter reduced interference from external sources to an acceptable level and the use of a tripolar recording configuration was not warranted. In addition the Humbug 50 Hz noise eliminators used in combination with the Faraday cage were effective in reducing interference from nearby electrical equipment and so no further processing was required. However VSD could be applied to double-differential, instead of single-differential signals.

At a first glance it appears that the VSD method increases the velocity selectivity of a VSR processor, as each AP has been assigned a singular velocity as opposed to a detailed velocity spectrum. It is important to understand that the VSD technique cannot increase velocity selectivity. The intrinsic selectivity has been shown to be a function primarily of the electrode geometry and the sample rate of the data acquisition system (Donaldson et al. 2008). VSD effectively quantises the peak of each IVS to a discrete velocity and associates with each velocity an amplitude proportional to the number of occurrences of that velocity in the data set. In addition the width of the bins of the histogram is pre-set to the velocity resolution of the system, 1 m/s in this case. As an example, if VSD were applied to the compound potentials recorded during electrical stimulation (as shown in figure 7), only the conduction

velocity with the largest amplitude, 14 m/s in this case, would be correctly identified. The results of electrical stimulation demonstrate the difficulty of isolating APs that are closely overlapping in time. VSD is better suited to sequences of non-overlapping APs where there is only a single peak within the IVS.

This limitation suggests an constraint on the maximum number of APs that may be correctly detected within a given time window. Recent experiments in microchannel structures for example have observed approximately 100 myelinated axons in a channel of dimensions $100\ \mu m^2$ (Chew et al. 2013). In this study individual axons were observed with relatively low firing rates and so the APs were well separated in time. However if all 100 axons were firing at10 Hz, for example, then the composite observed signal would contain 1000 APs/s and it is very likely that overlapping APs would occur. In this study the width of recorded APs was approximately 1 ms and so the theoretical, although statistically unlikely, limit for reliable detection is 1000 APs/s. In a practical application the size of fascicle that must be isolated in order to guarantee non-overlapping APs is related to two factors: the expected maximum firing rate of each axon and the number of axons within the fascicle. At present it is not known to what extent naturally occurring APs would overlap or to what extent this would ffect the methods proposed in this paper.

13. Applicability to Chronic Recordings

Hooks are inappropriate electrodes for chronic study but were chosen for this acute experiment to test the new VSD method. The use of hook electrodes provides time domain recordings with high SNR allowing AP propagation velocity to be calculated by hand and does not require custom-designed amplifiers. However, it should be noted that the signal processing techniques developed in this paper can be readily extended to MECs, provided that their lumens are small enough to give distinguishable spikes in the neurogram. Cuffs have a long proven history of stable chronic implantation in man (Polasek et al. 2009). Even more recent studies have shown that the use of *micro-channel nerve interfaces* that trap fine nerves or several separated fascicles should improve velocity selectivity, assuming more than three electrodes can be arranged in each channel (FitzGerald et al. 2012).

The signal processing methods used to implement VSR and VSD are, as already noted, fundamentally simple systems with the ability to be implemented in a low power real-time configuration. This is in contrast to existing neural recording systems that generally employ

statistical methods, termed ”spike sorting” such as *Principal Component Analysis* (PCA) and clustering. These methods not only require intensive computation but also cannot generally be operated in real-time since they require training (Gibson et al. 2012). The requirement for prior knowledge in spike sorting systems varies from one method to another, but generally speaking a good deal of information about the shape of the various AP waveforms is required before on-line processing can occur (Gibson et al. 2012). By comparison the VSD system described in this paper has a limited number of free variables, the width of the centroid filter (which is non-critical) and the noise floor of the recordings which can be estimated in real-time. VSR systems are therefore more suited to applications requiring implantation and real-time operation than approaches based on conventional pattern processing. A more detailed comparison of the implementation costs of the various methods is required before a definitive comparison can be made.

6. Conclusions

A method for extracting neuronal firing rates from physiological ENG based on conduction velocity has been demonstrated using *in-vivo* recordings in *rat*. Simple wire hook electrodes were used to form a short recording array in which a micro-dissected but intact fascicle was placed. Data were recorded using commercially available amplifiers and data converters before being processed using basic operations in MATLAB. This method generates a detailed overview of the firing rates of neurons based on their conduction velocity and direction of propagation. Changes within the firing rates for particular velocities were observed during both electrical and mechanical stimulation of the L5 dermatome and recorded signal amplitudes were sufficient to negate the use of averaging or more complex recording arrangements. Although it was shown that this method is directly applicable to physiological ENG, it remains to be investigated whether it is transferable to chronically implanted electrode structures such as cuffs or micro-channels.

7. Acknowledgments

This work was generously supported by the Brian Nicholson PhD scholarship.

8. References

Boretius T, Badia J, Pascual-Font A, Schuettler M, Navarro X, Yoshida K, et al. A transverse intrafascicular multichannel electrode (TIME) to interface with the peripheral nerve. Biosens Bioelectron [Internet]. Elsevier B.V.; 2010 Sep 15 [cited 2013 Aug 21];26(1):62–9. Available from: http://www.ncbi.nlm.nih.gov/pubmed/20627510

Carp JS, Tennissen AM, Wolpaw JR. Conduction velocity is inversely related to action potential threshold in rat motoneuron axons. Exp brain Res [Internet]. 2003 Jun [cited 2014 Jul 30];150(4):497–505. Available from: http://www.ncbi.nlm.nih.gov/pubmed/12715118

Chew DJ, Zhu L, Delivopoulos E, Minev IR, Musick KM, Mosse C a, et al. A microchannel neuroprosthesis for bladder control after spinal cord injury in rat. Sci Transl Med [Internet]. 2013;5:210ra155. Available from: http://www.ncbi.nlm.nih.gov/pubmed/24197736

Delivopoulos E, Chew DJ, Minev IR, Fawcett JW, Lacour SP. Concurrent recordings of bladder afferents from multiple nerves using a microfabricated PDMS microchannel electrode array. Lab Chip [Internet]. 2012 Jul 21 [cited 2014 Jul 13];12(14):2540–51. Available from: http://www.ncbi.nlm.nih.gov/pubmed/22569953

Donaldson N, Rieger R, Schuettler M, Taylor J. Noise and selectivity of velocity-selective multi-electrode nerve cuffs. Med Biol Eng Comput [Internet]. 2008 Oct [cited 2013 Jan 16];46(10):1005–18. Available from: http://www.ncbi.nlm.nih.gov/pubmed/18696136

Famm K, Litt B, Tracey KJ, Boyden ES, Slaoui M. Drug discovery: a jump-start for electroceuticals. Nature. 2013 Apr;496(7444):159–61.

FitzGerald JJ, Lago N, Benmerah S, Serra J, Watling CP, Cameron RE, et al. A regenerative microchannel neural interface for recording from and stimulating peripheral axons in vivo. J Neural Eng [Internet]. 2012 Feb [cited 2015 Jan 26];9(1):016010. Available from: http://iopscience.iop.org/1741-2552/9/1/016010

Gasser H. The classification of nerve fibers. Ohio J Sci [Internet]. 1941 [cited 2013 Sep 2];41(3):145–59. Available from: http://psycnet.apa.org/psycinfo/1942-00877-001

Gibson S, Judy JW, Markovic D. Spike Sorting: The First Step in Decoding the Brain: The first step in decoding the brain. IEEE Signal Process Mag [Internet]. 2012 Jan [cited 2015 Jan 26];29(1):124–43. Available from: http://ieeexplore.ieee.org/lpdocs/epic03/wrapper.htm?arnumber=6105476

Huang Y, Miller JP. Phased-array processing for spike discrimination. J Neurophysiol [Internet]. 2004 Sep [cited 2014 Dec 10];92(3):1944–57. Available from: http://www.ncbi.nlm.nih.gov/pubmed/15115796

Maynard EM, Nordhausen CT, Normann RA. The Utah Intracortical Electrode Array: A recording structure for potential brain-computer interfaces. Electroencephalogr Clin Neurophysiol [Internet]. 1997 Mar [cited 2015 Jan 26];102(3):228–39. Available from: http://www.sciencedirect.com/science/article/pii/S0013469496951760

Metcalfe B, Chew D, Clarke C, Donaldson N, Taylor J. An enhancement to velocity selective discrimination of neural recordings: Extraction of neuronal firing rates. Annu Int Conf IEEE Eng Med Biol Soc [Internet]. 2014 Aug [cited 2015 Jan 26];2014:4111–4. Available from: http://www.ncbi.nlm.nih.gov/pubmed/25570896

Milner-Brown H, Stein R, Yemm R. Changes in firing rate of human motor units during linearly changing voluntary contractions. J Physiol [Internet]. 1973 [cited 2014 Mar 13];371–90. Available from: http://www.ncbi.nlm.nih.gov/pmc/articles/PMC1350368/pdf/jphysiol00966-0117.pdf

Minev IR, Chew DJ, Delivopoulos E, Fawcett JW, Lacour SP. High sensitivity recording of afferent nerve activity using ultra-compliant microchannel electrodes: an acute in vivo validation. J Neural Eng [Internet]. 2012 Apr [cited 2014 Jul 27];9(2):026005. Available from: http://www.ncbi.nlm.nih.gov/pubmed/22328617

O'Mahony M. Sensory evaluation of food: statistical methods and procedures. CRC Press; 1986.

Pearson KG, Stein RB, Malhotra SK. Properties of action potentials from insect motor nerve fibres. J Exp Biol [Internet]. 1970 Oct;53(2):299–316. Available from: http://www.ncbi.nlm.nih.gov/pubmed/5481663

Polasek KH, Hoyen H a, Keith MW, Kirsch RF, Tyler DJ. Stimulation stability and selectivity of chronically implanted multicontact nerve cuff electrodes in the human upper extremity. IEEE Trans Neural Syst Rehabil Eng [Internet]. 2009 Oct;17(5):428–37. Available from: http://www.pubmedcentral.nih.gov/articlerender.fcgi?artid=2927980&tool=pmcentrez&rendertype=abstract

Rahal M, Winter J, Taylor J, Donaldson N. An improved configuration for the reduction of EMG in electrode cuff recordings: a theoretical approach. IEEE Trans Biomed Eng [Internet]. 2000 Sep [cited 2014 Dec 10];47(9):1281–4. Available from: http://europepmc.org/abstract/MED/11008430

Schalow G, Zäch G, Warzok R. Classification of human peripheral nerve fibre groups by conduction velocity and nerve fibre diameter is preserved following spinal cord lesion. J Auton Nerv Syst [Internet]. 1995 [cited 2013 Jan 29];1838(6). Available from: http://www.sciencedirect.com/science/article/pii/016518389400153B

Schuettler M, Donaldson N, Seetohul V, Taylor J. Fibre-selective recording from the peripheral nerves of frogs using a multi-electrode cuff. J Neural Eng [Internet]. 2013 Jun [cited 2014 Apr 11];10(3):036016. Available from: http://www.ncbi.nlm.nih.gov/pubmed/23640008

Schuettler M, Seetohul V, Rijkhoff NJM, Moeller F V, Donaldson N, Taylor J. Fibre-selective recording from peripheral nerves using a multiple-contact cuff: Report on pilot pig experiments. Conf Proc IEEE Eng Med Biol Soc [Internet]. 2011 Aug;2011:3103–6. Available from: http://www.ncbi.nlm.nih.gov/pubmed/22254996

Szűcs A. Applications of the spike density function in analysis of neuronal firing patterns. J Neurosci Methods [Internet]. 1998 [cited 2014 Dec 9];81:159–67. Available from: http://www.sciencedirect.com/science/article/pii/S0165027098000338

Taylor J, Donaldson N, Winter J. Multiple-electrode nerve cuffs for low-velocity and velocity-selective neural recording. Med Biol Eng [Internet]. 2004 Sep [cited 2014 Dec 10];42(5):634–43. Available from: http://link.springer.com/10.1007/BF02347545

Taylor J, Schuettler M, Clarke C, Donaldson N. A summary of the theory of velocity selective neural recording. Annu Int Conf IEEE Eng Med Biol Soc [Internet]. 2011 Jan [cited 2015 Jan 26];2011:4649–52. Available from: http://www.ncbi.nlm.nih.gov/pubmed/22255374

Taylor J, Schuettler M, Clarke C, Donaldson N. The theory of velocity selective neural recording: a study based on simulation. Med Biol Eng Comput [Internet]. 2012 Mar [cited 2012 Oct 8];50(3):309–18. Available from: http://www.ncbi.nlm.nih.gov/pubmed/22362024

Yoshida K, Jovanović K, Stein RB. Intrafascicular electrodes for stimulation and recording from mudpuppy spinal roots. J Neurosci Methods. 2000 Mar;96(1):47–55.